



Metrological sensitivity improvement of through-focus scanning optical microscopy by controlling illumination coherence

SHIN-WOONG PARK,¹ BYEONG GEON YOU,² GYUNAM PARK,² YOUNGBAEK KIM,³ JUNHO LEE,² JOONG HWEEO CHO,³ YUN YI,⁴ AND HWI KIM^{1,4,5,*}

¹*ICT Convergence Technology for Health & Safety, Korea University, 2511 Sejong-ro, Sejong 30019, South Korea*

²*Department of Optical Engineering, Kongju National University, 1223-24 Cheonan-daero, Seobuk-gu, Cheonan 31080, South Korea*

³*Department of Embedded Systems Engineering, Incheon National University, 119 Academy-ro, Yeonsu-gu, Incheon 22012, South Korea*

⁴*Department of Electronics and Information Engineering, Korea University, 2511 Sejong-ro, Sejong 30019, South Korea*

⁵*Department of Electrical and Computer Engineering, University of California, Davis, One Shields Avenue, Kemper Hall 2039, Davis, CA 95616, USA*

*hwikim@korea.ac.kr

Abstract: We investigate the influence of the degree of illumination coherence on through-focus scanning optical microscopy (TSOM) in terms of metrological sensitivity. The investigation reveals that the local periodicity of the target object is a key structural parameter to consider when determining the optimal degree of illumination coherence for improved metrological sensitivity. The optimal coherence conditions for the TSOM inspection of several target objects are analyzed through numerical simulation.

© 2019 Optical Society of America under the terms of the [OSA Open Access Publishing Agreement](#)

1. Introduction

Conventional high-numerical aperture (NA) optical microscopy is limited in resolution and depth-of-focus (DOF) when measuring high-aspect-ratio and nano-scale structures. Recently, through-focus scanning optical microscopy (TSOM) was proposed as a solution to this issue of optical microscopy [1,2]. The prominent feature of the TSOM which is contrast to the conventional optical microscopy is its computation-assisted indirect metrology scheme, which requires TSOM to computationally interpret a measured TSOM image by comparing it to an a priori prepared TSOM reference image database. In practice, differential TSOM images are analyzed in terms of mathematically designed measures to explicitly extract the structural features that they implicitly reflect. TSOM image databases are numerically constructed using finely modeled optical scattering simulators to create reference targets based on a range of structural parameters. TSOM image computation engines can also be constructed based on the finite difference time domain (FDTD) method, finite element method (FEM) or Fourier modal method (FMM).

To quantify the TSOM analysis, several quantitative measurement factors such as optical intensity range (OIR), different TSOM image (DTI), and mean square difference (MSD) are commonly used [1–6]. In practice, TSOM metrology uses MSD and OIR curves. In addition, the combined use of MSD and OIR can be used to determine the metrological information of the target sample. The difference of MSD becomes zero at the minimum point where the specification of the target sample is matched to a reference target in the TSOM image database. However, as the structural parameters deviate from the determination point, the MSD or OIR values move away from the minimum point where the structure is selected.

In order to commercialize TSOM technology, we need a reliable method of improving the sensitivity of TSOM measurement to more sensitively differentiate structural variations in the nano-structure sample than current state of the art systems can. Steeper curves of MSD or OIR in response to nanoscale structural variations in targets would be advantageous for measurement sensitivity. Sensitivity improvement in TSOM is made all the more critical by other variables, such as the quantization and inherent detection noise of the charge coupled device (CCD), smoothing out the meaningful signal variations in practice. Our previous work showed that TSOM images are very sensitive to the illumination numerical aperture (INA) and collection numerical aperture (CNA) of the TSOM system [7]. In optical metrology, the use of incoherent illumination is well established. Therefore incoherent illumination has been taken as a fixed instrumental condition even for TSOM metrology. The effect of the degree of illumination coherence on metrology performance has not been considered in previous works. However, it was perceived that the degree of illumination coherence is a crucial parameter when fitting the numerical TSOM model to accurately predict experimental TSOM images and that the value of MSD is influenced by the degree of illumination coherence [7]. Examining this point further, we could predict that the sensitivity of the MSD or OIR to structural variation can be improved by the adaptive control of the degree of coherence [7]. The optimal choice of degree of illumination coherence might lead to a significant performance improvement of TSOM metrology.

In this paper, we focus on the degree of illumination coherence and attempt to investigate the possibility of improving the sensitivity of TSOM using coherence-controlled illumination. This work is organized as follows. In section 2, TSOM images under coherent, incoherent, and partially coherent illumination are presented and the influence of the degree of illumination coherence on the TSOM image is elucidated. In section 3, the optimal conditions of illumination for various targets are specified and the relationship between the local periodicity of the target samples and the degree of illumination coherence is clarified in terms of sensitivity improvement. Finally, concluding remarks are given in section 4.

2. TSOM images under partially coherent illumination

The TSOM image under partially coherent illumination can be modeled by the Fourier modal method (FMM) as was proven in previous works [7–13]. The meaning of the essential parameters such as INA, CNA, and the degree of illumination coherence in the FMM model are depicted in Fig. 1.

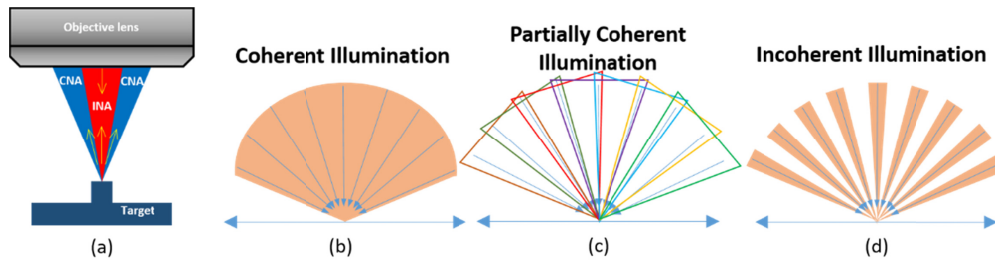


Fig. 1. (a) Schematic of an objective showing illumination and collection NA. Illustrations of the incident lighting case of (b) coherent, (c) partially coherent, and (d) incoherent illumination.

In the FMM framework, the reflective TSOM field under the partial coherent illumination is obtained by

$$|E_r| = \sqrt{\sum_{g=1}^G \left| \frac{1}{\text{deg}\#} \sum_{|g-g'| \leq \text{deg}\#} E_{r,g'} \right|^2}, \quad (1)$$

where deg\# is the parameter corresponding to the degree of coherence parameter. In our simulation setup, $\text{deg\#} = 0$ designates the incoherent field, while with $\text{deg\#} = \text{maximum value}$, the field is set to be coherent under the finite INA constraint. In these cases, the TSOM fields under the incoherent and coherent illuminations are represented by the discrete expression, respectively, by

$$|E_r| = \sqrt{\sum_{g=1}^G |E_{r,g}|^2} \quad (\text{incoherent illumination}), \quad (2)$$

and

$$|E_r| = \left| \sum_{g=1}^G E_{r,g} \right| \quad (\text{coherent illumination}), \quad (3)$$

These discrete representation of the coherent, partial coherent, and incoherent illuminations are correspondingly illustrated by Figs. 1(a), 1(b), and 1(c). The INA and CNA indicate the numerical aperture of the illuminating light and collection numerical aperture of the objective lens system, respectively. The FMM calculates the reflection and transmission fields under illumination of various degrees of coherence. In the case of coherent illumination, the entire light source is incident on one bundle, as illustrated in Fig. 1(b). In partially coherent illumination, each bundle of incident plane wave components of finite angular range is supposed to be internally coherent, but different bundles are incoherent with respect to each other. Figure 1(c) depicts multiple sets of narrow coherent converging beams incoherently illuminating the target sample. The angular width of the converging beam is determined by the degree of partial coherence. If the degree of coherence approaches complete incoherence, the incoherent illumination condition is represented by Fig. 1(d), where each plane wave component is statistically incoherent in the FMM. When the reflected diffraction fields of each coherent bundle are summed, the incoherent property is reflected. The scattering field induced by each coherent component in the illumination bundle is summed incoherently in the entire space. In [7], Park et al., the FMM model featuring incoherent illumination produce experiment-matched reliable numerical TSOM images. For successful TSOM metrology, the system parameters of INA, CNA, and the degree of illumination coherence in the TSOM model should be finely calibrated to match the numerical model to the actual experimental system.

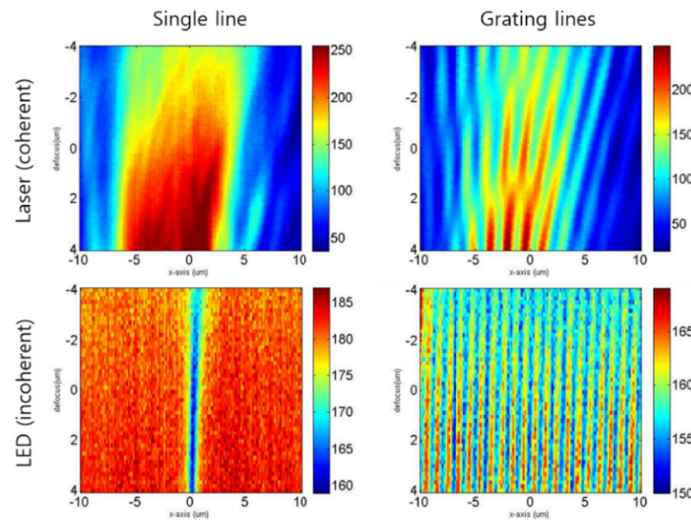


Fig. 2. TSOM images obtained with coherent and incoherent illumination conditions using an upgraded prototype of TSOM presented in ref [7].

The TSOM images acquired using the upgraded prototype of the TSOM system presented in ref [7], with coherent and incoherent illumination are shown in Fig. 2. The measured semiconductor structures are a single line with 160 nm width and grating lines with 160 nm width (800 nm pitch) of the same shapes as the structures 1 and 5 depicted in Fig. 4, respectively. As shown in the upper row in Fig. 2, when using a coherent laser source, it can be seen that the noise in the TSOM image is low, the TSOM image is clear and regular, and the total OIR is very high, which agrees with the simulation expectation in this paper. In particular, for grating lines on the right column in Fig. 2, the coherent TSOM image is expected to be more sensitive to the structural factors of a target sample than the incoherent TSOM image, because the lower-noise, clear and strong contrast TSOM image is obtained under the coherent illumination when the interval of the sample grating is sufficiently wide to have local periodicity. On the other hand, for a single line on the left column in Fig. 2, the diffraction pattern of the target sample region is clear and it is easy to distinguish in the case of the incoherent TSOM. This enables us to expect that the sensitivity of MSD is high when an incoherent light is considered for single lined structures. In this paper, we investigate the above expectation and the contrast point between single line and multiple lined structures regarding TSOM metrology by numerical simulation.

Figure 3 presents the effect of the degree of illumination coherence on the TSOM images, specifically the evolution of TSOM images of single- and multi-fin structures with a gradual change of illumination from perfectly incoherent illumination to perfectly coherent illumination. The TSOM images formed by illumination of different levels of coherency look quite different. The single-fin structure has the dimensions of 40 nm width and 100 nm height (Fig. 3(a)), while the multi-fin structure shown in Fig. 3(e) is specified by 160 nm width and 50 nm height, and 320 nm pitch. The corresponding TSOM images of the single fin and multi-fin sample structures under incoherent, partially coherent and coherent illumination are presented in Figs. 3(b)–3(d) and Figs. 3(f)–3(h), respectively. The TSOM images obtained using the incoherent light source shown in Figs. 3(b) and 3(f) are familiar that can be found in previous works [1–7]. The change due to increases in the degree of coherence is remarkable. Under the perfectly coherent lighting condition, the portion containing information in the TSOM image is highly concentrated, and as a result, the OIR is greatly increased. The TSOM image with partial coherence is an intermediate pattern between the incoherent and coherent TSOM images. The OIR is the absolute range of the differential signal normalized to perfect reflection of the incident illumination and increases from 26.58 to 99.88 and from 68.00 to 100.00 with incoherent and coherent lighting, respectively.

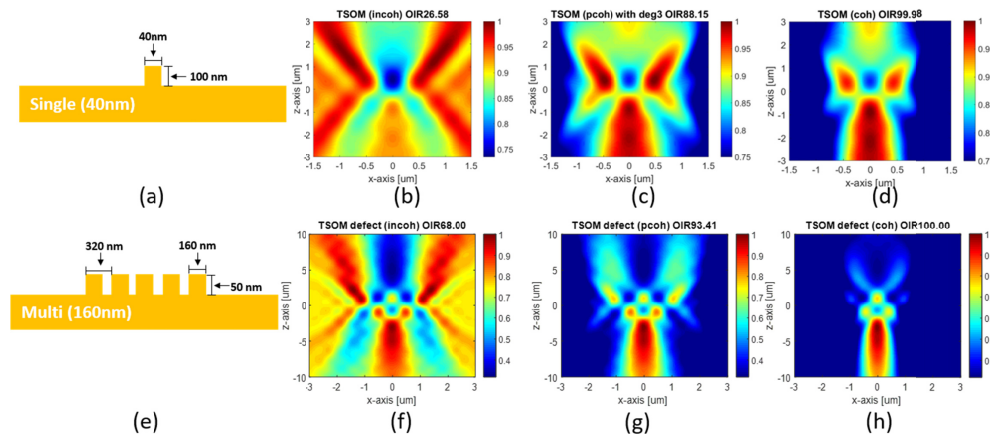


Fig. 3. TSOM images for the structures (a) and (e) according to the degree of coherence, incoherent: (b) and (f), partially coherent: (c) and (g), and coherent illumination: (d) and (h).

3. Effect of illumination coherence on TSOM measurement sensitivity

TSOM is indirect metrology using a numerical TSOM database and searching algorithm [14–16]. To quantify TSOM analysis, several quantitative measurement factors such as optical intensity range (OIR) different TSOM image (DTI), metric value (MV), and mean square difference (MSD) have been developed [1–6,14,16].

This study investigates changes in the sensitivity of the measurement factor, specifically MSD, according to the degree of coherence. The results can be used to determine the optimal conditions for TSOM inspection and measurement. Currently, semiconductor measurements using TSOM metrology are performed by a systematic comparison of DTI images using the MSD function of Eq. (4) and determination of the minimum value thereof [1–6,14],

$$MSD = \frac{1}{N} \sum_{i=1}^N (\text{TSOM}[\text{ref.}]_i - \text{TSOM}[\text{comp.}]_i)^2, \quad (4)$$

and the variation of the DTI without significantly changing its shape is quantified by the OIR [4,6],

$$OIR = \left[\begin{array}{l} \max(\text{TSOM}[\text{ref.}]_i - \text{TSOM}[\text{comp.}]_i | i = 1, 2, \dots, N) \\ - \min(\text{TSOM}[\text{ref.}]_j - \text{TSOM}[\text{comp.}]_j | j = 1, 2, \dots, N) \end{array} \right] \times 100 \quad (5)$$

where, TSOM[ref.] and TSOM[comp.] are the simulated TSOM images from the reference target and the target for comparison, and N is the total number of pixels in the image. In the TSOM system used for metrology, the reference image is one of the numerically constructed TSOM database images reflecting extremely fine structural variations in critical dimension (CD), height, pitch and so on. To determine the reference TSOM image that matches to the measured TSOM image, a parametric search is conducted by plotting the MSD while changing the structural parameters of the TSOM target structure and finding the reference TSOM image that minimizes the MSD. The parameters of that selected numerical TSOM image are then considered to be the measurement values of the real target structure. The issue is how sensitive is the MSD to variations in the structural parameters of the target structure [17,18].

OIR is a very simple definition which is the absolute difference in the maximum and minimum optical intensities present in a TSOM image or a DTI useful for quantitative comparison and MSD is the total deviation of the target TSOM and the reference TSOM. As seen in the mathematical definitions of MSD and OIR, the MSD senses the shape deviation of the TSOM image from the reference TSOM, while the OIR senses the deviation of light strength distribution contrast of the TSOM image. The single use of OIR does not differentiate two images because two images of totally different shapes can have the same OIR. But, for differentiating two images of extremely similar pattern, the OIR can be a reliable measure to index two images.

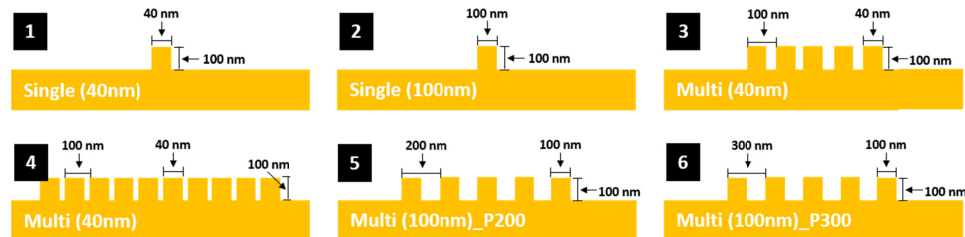


Fig. 4. Fin structures for numerical simulation.

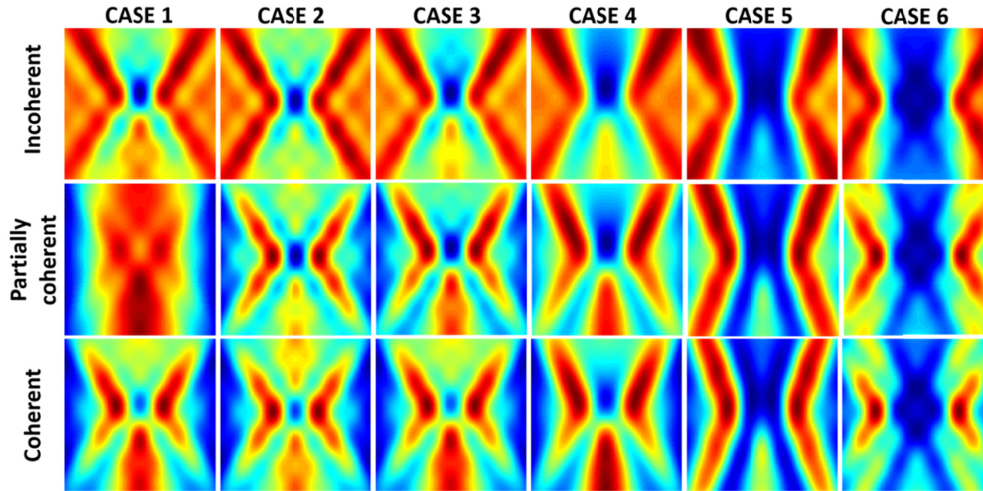


Fig. 5. TSOM images for the structural cases of Fig. 4 with the wavelength of 546nm, TM mode.

To numerically investigate this issue, we observe the MSD curves of the six simple Si fin structures presented in Fig. 4. All fin structures are 100nm tall. The first and second structures have one single fin with 40nm and 100nm widths, respectively. The third and fourth structures have five and ten fins with 40nm width and 100 nm period, respectively. The fifth and sixth structures have five fins of 100 nm width and wider periods of 200 nm and 300 nm, respectively. The incoherent, partially coherent, and coherent TSOM images for the six cases are presented in Fig. 5. In the simulation, the TSOM system is configured with the wavelength of 546nm, transversal magnetic (TM) mode, INA 0.1, and CNA 0.6.

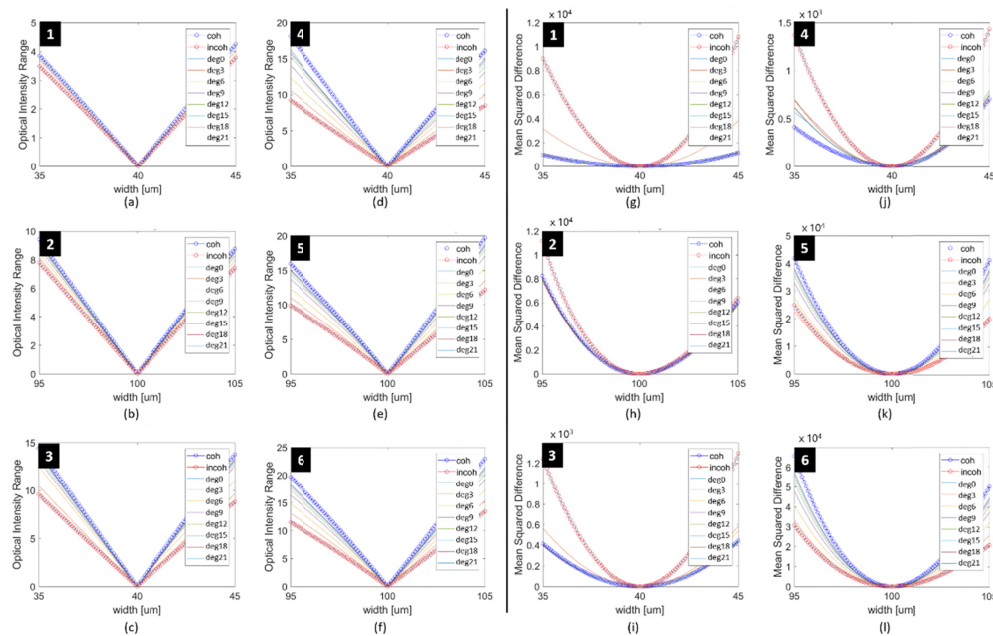


Fig. 6. The variation of the (a)-(f) OIR and (g)-(l) MSD curves of the six structures in Fig. 4.

For the simulation experiment, TSOM image databases of the six targets were created for three levels of illumination coherence: incoherent, partially coherent, and coherent modes. For the respective ten steps of degrees of coherence, two hundred TSOM images like those presented in Fig. 5 were created for DTI calculations, corresponding to fin widths varying in 0.1 nm steps. The DTI values were obtained from each database (DB) according to the reference widths of each structure, and their OIR and MSD values are plotted in Fig. 6 to compare the changes in those values. The differences in OIR values between the reference image and the DB image are calculated and those of the six target samples are shown in Figs. 6(a)–6(f) (left panel in Fig. 6). In the case of the OIR of the DTI images, it is apparent that the OIR of the coherent lighting is more sensitive than that of the incoherent lighting. The OIR values corresponding to partial coherence are in between those of the incoherence and coherence graphs, as shown in the Fig. 6. Considering the difference between the OIR graphs of the six samples, the larger the local periodicity, the more the difference between the absolute value of OIR and the OIR slope depends on the coherence. In the plots in Figs. 6(g)–6(l) (the right panel on Fig. 6), the structure is determined at the minimum value of the MSD curve.

As shown in Fig. 6, the OIR graph increases or decreases sharply and linearly, and the MSD graph has a parabolic curve pattern with a dip. Thus, the variation around the dip (sample space with extremely small structural change) is round. Thus the MSD cannot easily pinpoint the optimal point. At this microscopic tuning stage of analyzing very similar shaped structures with small MSD differences, the OIR may be useful to find the dip of the MSD curve. That is why previous TSOM papers recommend the combinatorial use of the MSD and OIR. In actual TSOM for metrology, the parabolic curve of the MSD value around the true value of the MSD is calculated, so the curvature value of the curve must be large. For example, considering cases 1 and 2 (40nm and 100nm single fin structures), we can see that the MSD sensitivity under incoherent illumination is better than that of coherent illumination with respect to the true reference value. In other words, the incoherent TSOM is more sensitive for structural changes in the single fin structures, so in such cases the use of incoherent illumination is preferable to coherent illumination. This is an important feature for increasing measurement accuracy and reinforcing robustness to noise in real TSOM systems. This tendency continues to the multi-fin structures in cases 3 and 4. Figures 6(i)–6(j) indicate that the MSD curves of the coherent cases tend to be lower than the curves of the incoherent cases. That is, the incoherent TSOM increases sharply with distance from the reference value. On the other hand, a notable switch is apparent in cases 5 and 6, in that the MSD curves of the coherent cases tend to be higher than the curves of the incoherent cases and the coherent TSOM increases more sharply with distance from the reference value.

In terms of MSD sensitivity, we can classify the six sample cases into two major categories, namely cases 1-4 and cases 5-6. The MSD of the first group showed higher sensitivity to incoherent illumination while the MSD of the second group exhibits higher sensitivity to coherent illumination. The physical origin of this noticeable difference can be qualitatively explained using the concept of local periodicity. Actually, for optical fields at 546nm, cases 3 and 4 of the first group can be seen as effective media [19]. Accordingly, cases 3 and 4 can be equivalently to a single fin structure with an effective permittivity. They are considered homogeneous structures without local periodicity or more generally, local corrugation. From hundreds of numerical simulations, we could infer that the MSD sensitivity of target structures with deep subwavelength structures that can be considered effective media is higher with incoherent illumination than coherent illumination. On the other hand, the structures of cases 5 and 6, feature a local periodicity, which results in a diffraction pattern due to the homogenization of the effective medium. In such cases, the MSD of DTI by coherent illumination is more sensitive. In the structure of case 3, the 100nm fin pitch is deep-subwavelength length and then appears to be an effective medium of 440nm total width rather than a periodic structure. In addition, the structures of cases 5 and 6 have respective 200 or

300 nm pitches, and in such situations, a type of crack exists in a homogeneous medium, which is more sensitive to coherent lighting. In the TSOM measurement of nanostructures, local periodicity is a criterion used to judge whether the structure can be considered as an effective medium and, therefore, which coherence level is more appropriate. According to our simulation research, this phenomenon was classified according to whether the total width of the structure is greater than 200 nm or not. This is because the sample can be recognized as an effective medium only when its critical feature is smaller than a certain size. Given this phenomenon, we can conclude that if the degree of coherence of illumination is adjustable, we can dramatically improve the sensitivity of the TSOM technique.

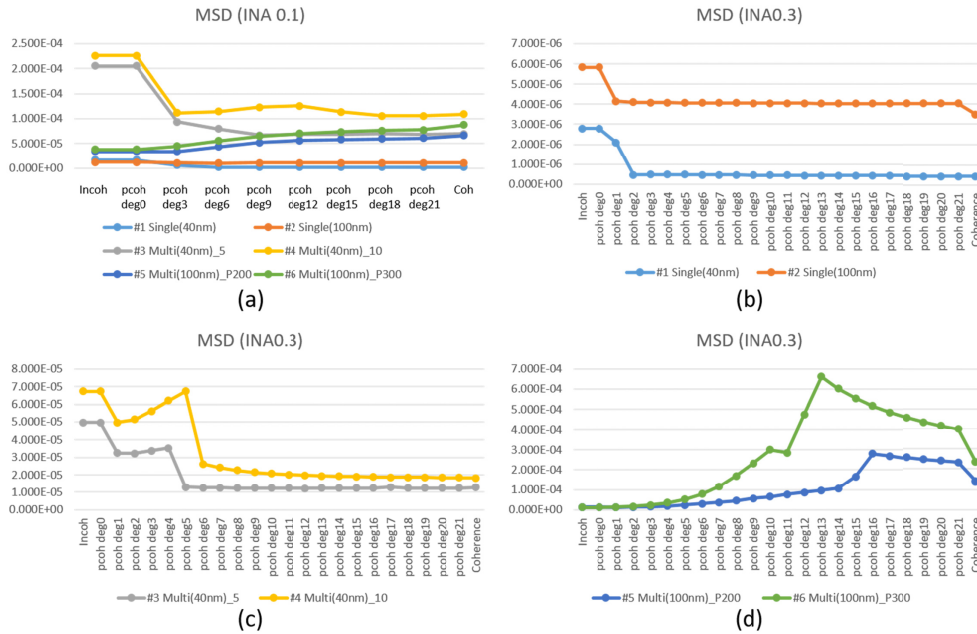


Fig. 7. MSD plots of the simulation structures: (a) INA 0.1 and (b)-(d) INA 0.3.

Figure 7 shows plots of the variations of MSD for the structures in Fig. 4 with changes in the degree of illumination coherence under the same conditions as in Fig. 6 (wavelength of 546nm, TM mode, INA 0.1 and 0.3, and CNA 0.6). In this simulation, the MSD values were calculated using comparative structures shifted extremely small 2 nm from the reference width, so structures with widths of 40 and 42 nm, and 100 and 102 nm were used for the comparison. As inferred in Fig. 6, the samples with a relatively large deviation from the reference sample shows the monotonic evolution the MSD curve. We tried to inspect the sample space close to the minimum deep of the MSD for the samples with tiny structural deviations. We found that the MSD value for a specific sample with extremely small 2nm deviation from the reference sample (near the widely round dip of the minimum spot of the MSD curve) does not change in a perfect monotonic increasing or decreasing pattern with changing the degree of coherence as presented in the simulation results of Fig. 7. Figure 7(a) shows the graphs of the MSD values of the six samples (with 42nm and 102nm widths) illuminated with fixed INA of 0.1 and changes in the degree of coherence. As the coherency changes from incoherence to coherence, the MSDs of cases 1-4 decrease, while the MSDs of cases 5-6 exhibit a slight increase. As the degree of coherence changes, the MSD values increase or decrease, and increased MSD means more sensitivity to structural variations at that degree of coherence. The variation of the MSD curves with INA 0.3 in Figs. 7(b)–7(d) show larger gaps between incoherence and coherence, but, nevertheless, present similar

characteristics in terms of sensitivity. The MSD is highest when incoherent lighting is applied to cases 1-4. In cases 5-6, (Figs. 7(a), 7(c), and 7(d)), it is noteworthy that the MSD value rises to its maximum value in a region of partial coherent lighting. In addition, for the non-effective medium samples in cases 5 and 6, in Fig. 7(d), the MSD curves are almost flat as the illumination changes from incoherent to partial coherent, but in the remaining cases 1-4 almost flat as it transitions from partially coherent to perfectly coherent. Moreover, comparing the data corresponding to the INA of 0.1 and 0.3, we can see that the sensitivity of the MSD is higher for coherent lighting when decreasing the INA. This phenomenon implies that the smaller INA with coherent lighting produces larger MSD values and higher sensitivity with non-effective medium samples of local periodicity. In other words, when the diffraction pattern due to the periodicity of the target structure appears in the TSOM image, the sensitivity for resolving structural discrepancies is high when coherent lighting is used. However, for the case of aperiodic deep-subwavelength effective medium structures, it is incoherent lighting that results in more sensitivity. Thus incoherent lighting is expected to be more advantageous for measurement of aperiodic structures.

4. Conclusion

In conclusion, we have shown the possibility of TSOM metrology sensitivity improvements through controlling the degree of the coherence of illumination. It is revealed that for the effective medium structures, including single fin and deep-subwavelength multi-fin structures, using incoherent illumination with high INA allows TSOM metrology to be more robust than using a high degree of coherent illumination. On the other hand, non-effective medium structures with local periodicity producing relatively strong interference in the scattering field are more sensitive to higher coherent illumination in terms of MSD. Elucidating an accurate interpretation of the relationship between the effective medium theory and the local periodicity of target structures in terms of quantitative criteria requires further theoretical research. In actual usage of the TSOM system, it is preferable to construct an appropriate adaptive illumination system capable of controlling the INA and of switching from partially coherent mode to incoherent mode according to the type of target sample. It is hoped that coherence-controlled TSOM will develop to become a high-performance in-line optical microscope inspection and metrology technique for state of the art semiconductor devices, such as the recent three-dimensional (3D) nanoscale semiconductor structures including silicon via (TSV) and fin field-effect transistors (Fin-FETs).

Funding

Ministry of Trade, Industry and Energy (MOTIE) and Korea Semiconductor Research Consortium (KSRC) (10048720); National Research Foundation of Korea (NRF) (NRF-2015R1C1A1A01054652).

References

1. R. Attota, R. Dixon, and A. Vladár, "Through-focus scanning optical microscopy," *Proc. SPIE* **8036**, 803610 (2011).
2. R. Attota, R. Dixon, J. Kramar, J. Potzick, A. Vladár, B. Bunday, E. Novak, and A. Rudack, "TSOM method for semiconductor metrology," *Proc. SPIE* **7971**, 79710T (2011).
3. R. Attota, D. G. Seiler, A. C. Diebold, R. McDonald, A. Chabli, and E. M. Secula, "TSOM method for nanoelectronics dimensional metrology," *AIP Conf. Proc.* **1395**, 57–63 (2011).
4. R. Attota, "Noise analysis for through-focus scanning optical microscopy," *Opt. Lett.* **41**(4), 745–748 (2016).
5. R. Attota and R. Silver, "Nanometrology using a through-focus scanning optical microscopy method," *Meas. Sci. Technol.* **22**(2), 024022 (2011).
6. R. Attota, B. Bunday, and V. Vartanian, "Critical dimension metrology by through-focus scanning optical microscopy beyond the 22nm node," *Appl. Phys. Lett.* **102**(22), 222107 (2013).
7. S.-W. Park, G. Park, Y. Kim, J. H. Cho, J. Lee, and H. Kim, "Through-focus scanning optical microscopy with the Fourier modal method," *Opt. Express* **26**(9), 11649–11657 (2018).
8. M. Pisarenco and I. Setija, "Alternative discretization in the aperiodic Fourier modal method leading to reduction in computational costs," *Proc. SPIE* **8789**, 87890K (2013).

9. H. Kim and B. Lee, "Mathematical modeling of crossed nanophotonic structures with generalized scattering-matrix method and local Fourier modal analysis," *J. Opt. Soc. Am. B* **25**(4), 518–544 (2008).
10. H. Kim and B. Lee, "Pseudo-Fourier modal analysis of two-dimensional arbitrarily shaped grating structures," *J. Opt. Soc. Am. A* **25**(1), 40–54 (2008).
11. H. Kim, I. M. Lee, and B. Lee, "Extended scattering-matrix method for efficient full parallel implementation of rigorous coupled-wave analysis," *J. Opt. Soc. Am. A* **24**(8), 2313–2327 (2007).
12. H. Kim, G. Park, and C. Kim, "Investigation of the Convergence Behavior with Fluctuation Features in the Fourier Modal Analysis of a Metallic Grating," *J. Opt. Soc. Korea* **16**(3), 196–202 (2012).
13. H. Kim, J. Park, and B. Lee, *Fourier Modal Method and Its Applications in Computational Nanophotonics* (CRC, 2012).
14. M. V. Ryabko, S. N. Koptyaev, A. V. Shcherbakov, A. D. Lantsov, and S. Y. Oh, "Method for optical inspection of nanoscale objects based upon analysis of their defocused images and features of its practical implementation," *Opt. Express* **21**(21), 24483–24489 (2013).
15. M. Ryabko, A. Shchekin, S. Koptyaev, A. Lantsov, A. Medvedev, A. Shcherbakov, and S. Y. Oh, "Through-focus scanning optical microscopy (TSOM) considering optical aberrations: practical implementation," *Opt. Express* **23**(25), 32215–32221 (2015).
16. R. Attota and J. Kramar, "Optimizing noise for defect analysis with through-focus scanning optical microscopy," *Proc. SPIE* **9778**, 977811 (2016).
17. R. K. Attota, P. Weck, J. A. Kramar, B. Bunday, and V. Vartanian, "Feasibility study on 3-D shape analysis of high-aspect-ratio features using through-focus scanning optical microscopy," *Opt. Express* **24**(15), 16574–16585 (2016).
18. R. K. Attota and H. Kang, "Parameter optimization for through-focus scanning optical microscopy," *Opt. Express* **24**(13), 14915–14924 (2016).
19. A. N. Norris, A. J. Callegari, and P. Sheng, "A generalized differential effective medium theory," *J. Mech. Phys. Solids* **33**(6), 525–543 (1985).